Rapid #: -8172749

Letter

Grazing incidence diffraction of cadmium arachidate multilayers at the solid-liquid interface

Chad E. Miller[I], Jaroslaw Majewski[II], Thomas Gog[III] and Tonya L. Kuhl*,[IV]

[I] Biophysics Graduate Group, University of California, Davis, California 95616, USA
[II] Manuel Lujan Neutron Scattering Center, Los Alamos National Laboratory, Los Alamos, New Mexico 87545, USA
[III] Advanced Photon Source, Argonne National Laboratory, Argonne, IL 60439, USA
[IV] Department of Chemical Engineering and Material Science, University of California, Davis, California 95616, USA

Grazing incidence diffraction / X-ray reflectivity /
Thin organic films / Solid-liquid interface / Multilayers /
Cadmium arachidate

Abstract. Using complementary X-ray reflectivity (XR) and grazing incidence X-ray diffraction (GIXD), we report structural studies of supported thin-organic layers in contact with water and air. Using a monochromatic synchrotron beam to penetrate 10 mm of liquid, we have characterized buried films composed of 12.5 repeating bilayers of arachidic acid ($C_{20}H_{40}O_2$) complexed with cadmium ions (cadmium arachidate, $CdAr_2$). We found that the layered structure of the $CdAr_2$ multilayers do not exhibit rearrangement after exposure to water with negligible water penetration into the inner layers when compared to their dry state. These findings are consistent with the formation of extremely robust $CdAr_2$ multilayers that can withstand multiple rinses in strong organic solvents, acid, and mechanical wear. The second goal was to demonstrate the feasibility of similar experiments to study much thinner single bilayer bio-membranes. These studies are the first successful GIXD experiments of ultra thin-organic film composed of a few layers at the solid-liquid interface.

Introduction

A current trend in interfacial science is the utilization of ultra thin organic films, including single bio-membranes, which are structurally ordered on the molecular level. These films usually involve molecules that assemble into ordered films at the solid-air or solid-liquid interface. Potentially, ordered organic films may have applications in nonlinear optics [1], molecular electronics, chemical/biochemical sensors, and surface patterning [2]. Maintaining the structural integrity of these ordered films when exposed to bulk solvents or wet environments will further enhance their utility. As a result, understanding their physical properties under various conditions is vital.

A great deal of work has been done to characterize such ordered films at the solid-air or air-liquid interfaces [3, 4]. In particular, X-ray reflectivity (XR) and grazing incidence diffraction (GIXD) using synchrotron X-ray radiation have unique capabilities for determining the spatial organization of organic thin films with almost angstrom resolution [5]. Unfortunately, due to absorption and diffuse scattering by water, it is not clear that the GIXD signal would be sufficient to characterize the structure of ordered films composed of only a few multilayers in contact with liquid. In this work, we report the first successful GIXD experiments of a thin-organic film composed of 12.5 repeating $CdAr_2$ bilayers at the solid-liquid interface in water.

These successful investigations of 12.5 $CdAr_2$ bilayers allude to the feasibility of using GIXD to study solid-supported single bilayer membranes at the solid-liquid interface. Recent work has shown that GIXD can be used to study highly-oriented, phospholipid multilayers composed of thousands of bilayers in humid environments [6, 7]. It is known that stacked lipid membrane lamella have different structural characteristics than single membranes in contact with a solid support. Therefore, it is imperative to study the in-plane structure of single bilayers due to their more relevant application in biomembrane sensors.

Materials and methods

Cadmium arachidate multilayers were prepared by conventional Langmuir-Blodgett (LB) deposition [8]. Arachidic acid ($C_{20}H_{40}O_2$) dissolved in chloroform (1 mg/mL) was spread on a subphase consisting of Millipore water with 1 mM $CdCl_2$ and 10 mM ACES buffer (pH 6.8). The dipping process was performed at a constant surface pressure

* Correspondence author (e-mail: tlkuhl@ucdavis.edu)

(30 mN/m) and dipping speed (5 mm/min). The monolayers were deposited on polished substrates made of single-crystal quartz. Before deposition, the substrates were submerged in a freshly made piranha acid bath (70% sulfuric acid, 30% H_2O_2) for 15 minutes and then cleaned with UV ozone for 10 minutes. The substrates were pulled through the interface 25 times, starting in the subphase and ending in air. The transfer ratio was equivalent for all 25 depositions, confirming uniform stacking of monolayers. When measuring at the solid-liquid interface, the samples were submerged in water or buffer on a time scale of 1–2 hours prior to exposure to X-rays.

X-ray reflectivity

All synchrotron X-ray measurements were carried out using the 6-circle diffractometer at the ID-9 (undulator) CMC-cat beam line at the Advanced Photon Source (APS), Argonne National Laboratory (ANL) (Argonne, IL). The synchrotron X-ray beam was monochromated to a wavelength of 0.69 Å (18 keV) by a cryogenic Kohzu double crystal monochromator containing a feedback loop with a position sensitive ion-chamber in front of the sample for beam position stability. We used single crystal quartz substrates with dimensions 10×50 mm^2 as the solid support. After CdAr$_2$ deposition the substrate was placed in a water filled, stainless steel cell (with Kapton windows) and oriented so that the 10 mm dimension was along the X-ray beam. The 18 keV photons penetrated through the 10 mm thick water layer with a transmission of approximately 40%. The small sample size (along the dimension of the beam) and need for the beam to strike at very low angles required ultra high precision, fixed slits (170 μm molybdenum) to define the vertical dimension of the X-ray beam. The horizontal slit opening was 1 mm. Using the above setup, we measured the reflectivity from substrate-supported CdAr$_2$ multilayers out to a momentum transfer of about 0.8 Å^{-1} covering almost 10 orders in dynamic range of intensity with reasonable statistics. Typical scanning times for this q_z range were 10 minutes. The reflected X-rays were counted using a NaI scintillation detector. Error bars on the data represent the statistical errors in the measurements (standard deviation, σ_R). Since at low angles the footprint of the beam is bigger than the size of the quartz substrate the measured reflectivities have been corrected for this effect.

Reflectivity, R, is defined as the intensity ratio of X-rays specularly scattered from the surface relative to the incident X-ray beam intensity. When measured as a function of wave-vector transfer ($q_z = |k_{out} - k_{in}| = 4\pi \sin \theta/\lambda$, where θ is the angle of incidence and λ is the wavelength of the X-ray beam, see Fig. 1), the reflectivity curve contains information regarding the sample-normal profile of the in-plane average of the coherent scattering length densities. By modeling the deviation of the measured specular X-ray reflectivity from Fresnel's law for a perfect interface, detailed information on the average electron density distribution in the direction normal to the interface can be determined. Analysis of the measured reflectivity curves was performed by dividing the structural components of the system (along the substrate normal)

into homogeneous slabs or boxes of constant electron density. These boxes, which physically represent different portions of the cadmium arachidate layers (hydrocarbon tails and $CO_2^- - Cd - CO_2^-$ headgroups), were then refined using the Parratt formalism [9] and least-squared minimization method. The uncertainty in the momentum transfer vector, $\Delta q_z = 0.003$ Å^{-1}, was included in the data fitting. This analysis provides the thickness of each layer (box), electron density ($e(z)$), and adjacent interfacial Gaussian roughness (σ), to account for roughening at the boundary due to static or thermal roughness. Consequently, the structural components perpendicular to the interface can be resolved.

Grazing incidence diffraction

At the air-water interface, prior to LB deposition onto the solid substrate, each of the deposited CdAr$_2$ monolayers is composed of 2D ordered domains with random orientation about the direction normal to the subphase surface, and can therefore be described as a 2D powder [10, 11]. Due to the nature of the LB procedure and the presence of the quartz support, the deposited CdAr$_2$ layers orient into lamellas parallel to the substrate. For the GIXD experiments (Fig. 1), the X-ray beam was adjusted to strike the surface at an incident angle of 0.05°, which corresponds to the vertical momentum transfer vector $q_z = 0.625 q_c$, where $q_c = 0.0254$ Å^{-1} is the critical scattering vector for total external reflection for quartz submerged in water (e-densities of quartz and water are 0.84 e^-/Å^3 and 0.33 e^-/Å^3, respectively). At this angle the incident wave is totally reflected, while the refracted wave becomes evanescent traveling along the substrate surface. Such a configuration maximizes surface sensitivity. GIXD geometry is shown Fig. 1. The dimension of the incoming X-ray beam footprint on the quartz surface was approximately 1 mm × 10 mm. For in-plane diffraction measurements, a NaI scintillation counter was placed behind adjustable slits on a translational stage (moving in-plane with the substrate interface
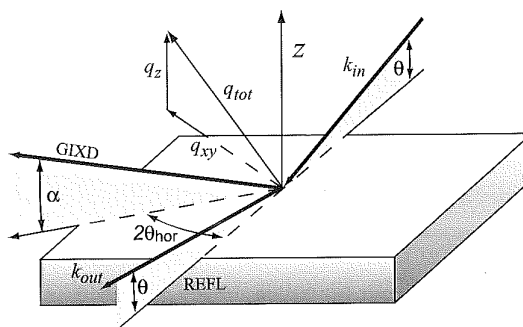

Fig. 1. Scattering geometry for grazing incidence diffraction (GIXD) and X-ray Reflectivity (XR). For GIXD, the angle of incidence, θ, of the X-ray beam is less than the angle of total external reflection from the substrate in contact with the superstrate (water or air). k_{in} and k_{out} are the wave vectors of the incident and reflected beams. The scattering vector $q_{xy} \approx 4\pi \sin \theta_{hor}/\lambda$ is parallel to the substrate plane and $q_z = 2\pi \sin \alpha/\lambda$ is perpendicular to it. For reflectivity measurements, $2\theta_{hor}$ is equal to zero and the intensity is recorded as a function of angle θ in specular geometry.

along the $2\theta_{\mathrm{hor}}$ angle) covering a q_{xy} range of 1.3 Å^{-1} to 1.9 Å^{-1}. For rod scans (scans along q_z vector), the in-plane scattering angle was kept fixed at the position of maximal Bragg intensity and the height of the NaI detector above the surface was varied. The vertical slit opening of 1mm in front of the detector determined the q_z resolution of 0.013 Å^{-1}.

For the collection of diffracted intensities, a scintillation NaI detector with slits in front of it was used. The slits were adjusted to give the horizontal resolution of the measurement (along the quartz surface), $FWHM_{\mathrm{resol}}$ $(q_{xy}) = 0.0084$ Å^{-1}. The scattered intensity was measured by scanning over a range of the horizontal scattering vector component, q_{xy} (or $q_{\parallel}$) $\cong (4\pi/\lambda) \sin(2\theta_{\mathrm{hor}}/2)$, where $2\theta_{xy}$ is the angle between the incident and diffracted beam projected onto the horizontal quartz plane. Such a scan, integrated over the vertical acceptance of the slit (0.042 Å^{-1}) along the q_z direction, yields in-plane *Bragg peaks* (Fig. 3a). Conversely, the scattered intensity recorded with narrow vertical slits of the resolution $FWHM_{\mathrm{resol}}(q_z) = 0.013$ Å^{-1} along q_z ($q_z = q_{\perp} = (2\pi/\lambda) \sin(\alpha)$), where α is the exit angle measured from the surface of the substrate) produced q_z-resolved scans called *rod scans* (Figs. 3b, c). *Rod scans* where measured at the scattering vector q_{xy} corresponding to maximum intensity of the in-plane Bragg peak and background subtracted. The scattering of X-rays along rods perpendicular to the quartz substrate reflects the presence of well-oriented (textured) lamellas of CdAr$_2$. The intensity distribution along the in- and out-of-plane Bragg peaks can be analyzed to yield information on the packing of the cadmium arachidate molecules. The positions $q_{\mathrm{tot}} = (q_{xy}^2 + q_z^2)^{1/2}$ of the Bragg peaks allow the determination of the d-spacings, $d = 2\pi/q_{\mathrm{tot}}$, for the 3D lattice and calculation of the 3-D unit cell dimensions. The width of the Bragg peaks corrected for the instrumental resolutions, give the finite size of the crystalline domains in the direction of the reciprocal scattering vector q_{xy} (the 2D in-plane crystalline coherence length, L_{xy}) and in the direction perpendicular to it (out-of-plane crystalline coherence length, L_z) according to the Scherrer formula: $L_{xy,z} \cong 0.9[2\pi/FWHM_{\mathrm{intrinsic}}(q_{xy,z})]$ where $FWHM$ are the corresponding full width at half maximum heights of the peaks [12]. The intrinsic FWHM can be obtained using the equation:

$$FWHM_{\mathrm{intrinsic}}(q_{xy,z}) = [FWHM_{\mathrm{meas}}(q_{xy,z})^2$$
$$- FWHM_{\mathrm{resol}}(q_{yx,z})^2]^{1/2}.$$

Beam damage

As a precaution against beam damage, in XR the sample was frequently translated by 2 mm, in the horizontal plane, perpendicular to the incoming beam. Re-recording part of the reflectivity curve before and after translation afforded a check of the reproducibility. During reflectivity, the maximum dose of X-rays was estimated by the equivalent number of seconds exposed to the direct, un-attenuated beam. Similarly, translation of the sample by 2 mm was performed between GIXD scans. The total scan time for a single GIXD scan was approximately 2 minutes.

Results

Reflectivity

Comparison of reflectivity profiles of supported CdAr$_2$ multilayers in air and water (Fig. 2) demonstrates no significant change in the position or intensity of the peaks. The same box model, adjusted only for differences in the electron density of the superstrate, air *vs.* water, fits both reflectivity profiles. This finding demonstrates that the multilayer structure is not significantly altered by submersion in water. The solid line (Fig. 2a) is the calculated reflectivity for a multilayer structure composed of 45.8 Å thick hydrocarbon bilayers (22.9 Å per monolayer, $\rho_e = 0.298\ e^-/$Å^3) separated by 9.7 Å thick headgroup/cadmium/headgroup layers (CO$_2^-$–Cd–CO$_2^-$, $\rho_e = 0.447\ e^-/$Å^3). The hydrocarbon layer represents two arachidic acid chains in a tail–to-tail configuration (Fig. 2b). A fully stretched 19-carbon chain extends approximately 24 Å (1.26 Å/Carbon). As reflectivity is sensitive to the density distribution normal to the surface the model thickness of 22.9 Å suggests that the hydrocarbon tails are tilted ~17° with respect to the surface normal. The ob-
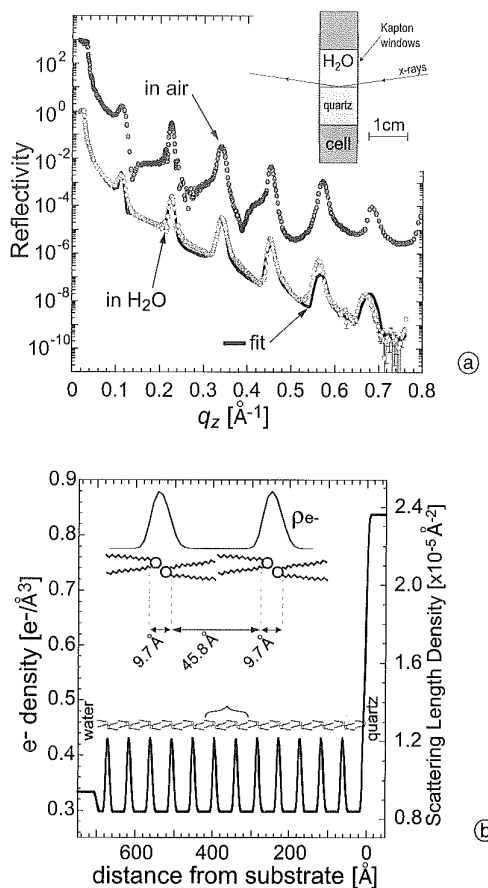

Fig. 2. (a) Reflectivity versus q_z for 12.5 cadmium arachidate bilayers in air and in H$_2$O. The fit (solid line) is the calculated reflectivity for a multilayer structure with a 45.8 Å hydrocarbon layer (0.298 $e^-/$Å^3) separated by a 9.7 Å headgroup/cadmium layer (0.447 $e^-/$Å^3). There is not a significant difference in the position and intensity of the Bragg reflections of the multilayer sample before and after submersion in H$_2$O. The reflectivity in air is offset by 1000 for clarity. (b) The obtained e-density distribution of 12.5 bilayers of CdAr$_2$.

tained *e*-density (0.298 $e^-/\text{Å}^3$) and thickness for the hydrocarbon tail region corresponds to an average area per molecule of 22.4 Å^2. Based on this number and the fitted *e*-density of the headgroup region (0.447 $e^-/\text{Å}^3$) we can estimate that on average there are 1.1–1.2 Cd^{2+} ions per two CO_2^- headgroups. The consistency in the *e*-density of the tails in air and water indicates that there is no water penetration into the interior of the hydrocarbon bilayers. Based on the reflectivity data we can calculate the volume fraction averaged *e*-density of CdAr$_2$ multilayers. The obtained value of 0.324 $e/\text{Å}^3$ is less than the electron density of water (0.33 $e/\text{Å}^3$).

Grazing incidence diffraction

The GIXD from 12.5 bilayers of cadmium arachidate (CdAr$_2$) at the solid-water interface is shown in Fig. 3a. Two peaks with Miller indices of $(1, 1, l)$ and $(0, 2, l)$ are clearly resolved along the q_{xy} vector. Analysis of the Bragg peak positions are summarized in Table 1 and 2 and reveal an orthorhombic unit cell of dimensions: $a = 4.86$ Å,

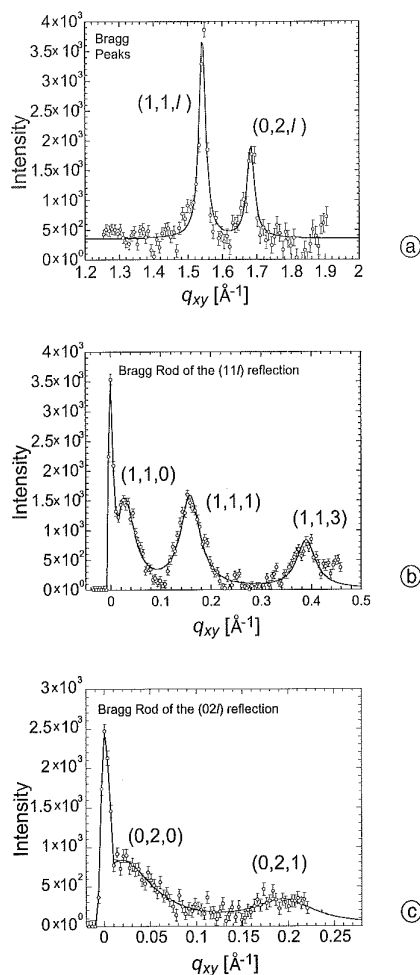**Table 1.** Parameters obtained from in-plane GIXD scans.

Cd-arachidate	q_{xy} positions (Å^{-1})	*d*-spacing (Å)	peak FWHM (Å^{-1})	Coherence length, L_{xy} (Å)
$(1, 1, l)$	1.542	4.08	0.023	260
$(0, 2, l)$	1.683	3.73	0.026	230

$b = 7.45$ Å, $c = 48.82$ Å. These values are in agreement with previous work in air [13, 14]. There are four molecules per unit cell where the projection of the area on the a, b plane occupied by one molecule is equal to 18.2 Å^2. This is in contrast to an overall average molecular area of 22.4 Å^2 from reflectivity measurements and shows that the crystalline (diffracting) domains pack more efficiently. Moreover, the volume fraction of disordered CdAr$_2$ phase is significant. The in-plane coherence lengths, L_{xy}, were 260 Å and 230 Å for the $(1, 1, l)$ and $(0, 2, l)$ Bragg peaks, respectively. These in-plane coherence lengths correspond to approximately 45 to 50 molecules in positional, in-plane, registry.

The $(1, 1, l)$ rod scan is shown in Fig. 3b. The $(1, 1, 0)$, $(1, 1, 1)$, and $(1, 1, 3)$ Bragg reflections can be clearly resolved along the q_z vector. The $(0, 2, l)$ rod scan is shown in Fig. 3c. Analysis of the all measured Bragg rods is summarized in Table 2. The out-of-plane coherence lengths, L_z, for the $(1, 1, 0)$ $(1, 1, 1)$ $(1, 1, 3)$, $(0, 2, 0)$ and $(0, 2, 1)$ reflections are much smaller than the depth of penetration of the X-ray beam (Fig. 4b) and smaller than the corresponding in-plane coherence lengths. Along the $(1, 1, l)$ rod, the coherence length (L_z) is equal to 130 Å, which, on average, is equivalent to approximately 2.7 CdAr$_2$ bilayers of the multi-lamellar film in positional registry. Along $(0, 2, l)$ rod this number ($L_z = 70$ Å) deceases even further to approximately 1.4 bilayers. The difference in the L_z of the $(1, 1, l)$ and $(0, 2, l)$ rod scans is most likely due to more disorder of the CdAr$_2$ molecules perpendicular to the $(0, 2, 0)$ plane. Since the maximum of the $(1, 1, 0)$ reflection is slightly off from $q_z \approx 0$ Å^{-1} and the maximum of the $(0, 2, 0)$ reflection coincides with $q_z \approx 0$ Å^{-1}, the molecules are slightly tilted towards the a-axis of the unit cell in the plane spanned by the **a** and **c** vectors. These off horizon reflections are consistent with the molecular tilt observed by the reflectivity data.

Our results for CdAr$_2$ multilayers at the solid liquid interface compare very well to GIXD measurements of 21 monolayers of CdAr$_2$ at the solid-air interface per-

Fig. 3. Grazing incidence diffraction (GIXD) of 12.5 bilayers of cadmium arachidate (CdAr$_2$) at the quartz-water interface. (**a**) Bragg peak positions are in excellent agreement with those obtained at the solid-air interface showing that there is no significant rearrangement of the layers when exposed to water. (**b**) and (**c**) show the $(1, 1, l)$ and $(0, 2, l)$ *rod scans*, respectively, of the peaks in (a).

Table 2. Parameters obtained from out-of-plane GIXD scans.

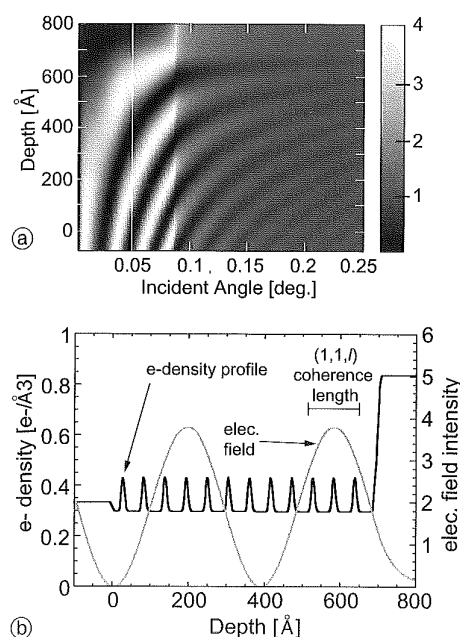| Cd-arachidate	q_z positions (Å^{-1})	peak FWHM (Å^{-1})	Coherence length, L_z (Å)
$(1, 1, l)$			
$(1, 1, 0)$	0.028	0.046	130
$(1, 1, 1)$	0.158	0.046	130
$(1, 1, 3)$	0.389	0.046	130
$(0, 2, l)$			
$(0, 2, 0)$	0.019	0.081	70
$(0, 2, 1)$	0.195	0.078	70

Fig. 4. (a) Distribution of the intensity of electric field at the water/CdAr₂/quartz interface as a function of incidence angle, θ, and the depth of the system. The critical angle of quartz in contact with water is ~0.0835°. A depth of 0 Å corresponds to the water in contact with CdAr₂ and 800 Å corresponds to the quartz support. The brightness table shows the intensity of the standing wave inside the system. An intensity of 1 corresponds to the intensity of the incoming X-ray beam. (b) Comparison of the intensity of the electric field at an incident angle $\theta = 0.05°$ (the angle of incidence used in our experiments shown by a white vertical line in Fig. 4a) and the distribution of the electron density of CdAr₂ in contact with water.

formed by Tippman-Krayer *et al.* [14]. Both Bragg peaks and Bragg rods match, showing that there is no significant rearrangement of the CdAr₂ layers when exposed to water. This finding is also consistent with our reflectivity results showing no water penetration into inner layers. The intensity distribution between the (1, 1, *l*) and (0, 2, *l*) rod scans also compare favorably with the work of Tippman-Krayer *et al.*, suggesting that there is a $^{1}/_{4}$ of a unit cell displacement of the consecutive layers along the *a*-axis of the bilayers.

In our case the *c*-dimension of the unit cell is smaller than that reported by Tippman-Kayer *et al.* This indicates that the molecular tilt is bigger in our case, perhaps due to the difference in the LB deposition protocol.

Since the averaged electron density of CdAr₂ is less than the electron density of water there is no total reflection when the X-ray beam passes from liquid into the multilayers. An incident angle of 0.05° guarantees almost full illumination of the structure normal to the interface. However, in order to understand the exact distribution of the electric field as a function of depth inside the CdAr₂ multilayer structure, we recursively calculated the electric field using Parratt's method [9, 15]. This calculation was based on the electron density distribution obtained from reflectivity measurements. Due to the interference between transmitted and reflected beams within the film, standing waves are present as function of incident angle and the distance along the sample normal (Fig. 4a).

Below the critical angle of quartz in contact with water (~0.0835°), strong interference leads to large oscillations of the electric field intensity — *i.e.* the standing wave. Figure 4b shows the real space comparison of the electron distribution of the CdAr₂ multilayers and the calculated intensity of X-ray electric field. Approximately 70% of the total thickness of the CdAr₂ multilayers (~500 Å) experiences X-ray electric field intensities greater than the intensity of the incoming beam. Figure 4b also illustrates that the maximum out-of-plane coherence length (130 Å) obtained in the experiment is less than the depth of the illuminated portion of the structure.

Discussion/conclusions

Many biological applications require the structure of assembled layers to be maintained when exposed to an aqueous phase. This necessitates the ability to characterize these thin-films at the solid-liquid interface since layers may have different properties when in contact with water. We have shown that the structure of 12.5 CdAr₂ bilayers is preserved after submersion in water with no water penetration into the interior of the layers.

According to our knowledge, this is the first GIXD measurement at the solid-liquid interface of a sample that wasn't composed of "thousands" of layers. Several studies pursuing the GIXD of these much thicker multilayer systems have been successful in very humid environments [6, 7]. With careful improvements to our studies, 12.5 bilayers will be decreased to a single bilayer, enabling the measurement of single biomembranes on a solid support in contact with water. A thorough working knowledge of the lateral organization of solid-supported single bilayers will aid the development of biomembranes sensors.

References

[1] Wang, H.; Chiarelli, P. A.; Liu, D.; Robinson, J. M.; Casson, J. L.; Majewski, J.: Pacific Rim Conference on Lasers and Electro-Optics. Taipei, Taiwan, 2003, Vol. 2, p. 557.
Li, D. Q.; Ratner, M. A.; Marks, T. J.; Zhang, C. H.; Yang, J.; Wong, G. K.: Chromophoric Self-Assembled Multilayers – Organic Superlattice Approaches to Thin-Film Nonlinear Optical-Materials. J.A.C.S. **112** (1990) 7389–7390.
[2] Roberts, G. G.: An Applied Science Perspective of Langmuir-Blodgett Films. Adv. Physics **34** (1985) 475–512.
[3] Helm, C. A.; Möhwald, H.; Kjaer, K.; Als-Nielsen, J.: Phospholipid Monolayers between Fluid and Solid States. Biophys. J. **52** (1987) 381–390.

[4] Miller, C. E.; Majewski, J.; Faller, R.; Satija, S.; Kuhl, T. L.: Cholera toxin assault on lipid monolayers containing ganglioside GM(1). Biophys. J. **86** (2004) 3700–3708.

[5] Als-Nielsen, J.; Jacquemain, D.; Kjær, K.; Leveiller, F.; Lahav, M.; Leiserowitz, L.: Principles and applications of grazing incidence X-ray and neutron scattering from ordered molecular monolayers at the air-water interface [review]. Phys. Rev. Lett. **246** (1994) 252–313.

[6] Munster, C.; Lu, J.; Schinzel, S.; Bechinger, B.; Salditt, T.: Grazing incidence X-ray diffraction of highly aligned phospholipid membranes containing the antimicrobial peptide magainin 2. Eur. Biophys. J. Biophy. **28** (2000) 683–688.

[7] Spaar, A.; Munster, C.; Salditt, T.: Conformation of peptides in lipid membranes studied by X-ray grazing incidence scattering. Biophysical J. **87** (2004) 396–407.

[8] Takamoto, D. Y.; Aydil, E.; Zasadzinski, J. A.; Ivanova, A. T.; Schwartz, D. K.; Yang, T. L.; Cremer, P. S.: Stable ordering in Langmuir-Blodgett films. Science **293** (2001) 1292–1295.

[9] Parratt, L. G.: Surface Studies of Solids by Total Reflection of X-Rays. Phys. Rev. **95** (1954) 359–369.

[10] Leveiller, F.; Bohm, C.; Jacquemain, D.; Mohwald, H.; Leiserowitz, L.; Kjær, K.; Alsnielsen, J.: 2-Dimensional Crystal-Structure of Cadmium Arachidate Studied by Synchrotron X-Ray-Diffraction and Reflectivity. Langmuir **10** (1994) 819–829.

[11] Leveiller, F.; Jacquemain, D.; Lahav, M.; Leiserowitz, L.; Deutsch, M.; Kjaer, K.; Alsnielsen, J.: Crystallinity of the Double-Layer of Cadmium Arachidate Films at the Water-Surface. Science **252** (1991) 1532–1536.

[12] Guinier, A.: X-ray diffraction in crystals, imperfect crystals, and amorphous bodies (W. H. Freeman, ed.) San Francisco, 1963.

[13] Vitta, S.; Metzger, T. H.; and Major, S. S.: Structural assembly of Cd-arachidate molecules in multilayers. J. Chem. Phys. **111** (1999) 11088–11094.

[14] Tippmann-Krayer, P.; Kenn, R. M.; and Möhwald, H.: Thickness and Temperature-Dependent Structure of Cd-Arachidate Langmuir-Blodgett-Films. Thin Solid Films **210** (1992) 577–582.

[15] Tolan, M.: X-ray scattering from soft-matter thin films — Materials science and basic research — Introduction. Springer Tr. Mod. Phys. **148** (1999) 1.

ZEITSCHRIFT FÜR KRISTALLOGRAPHIE
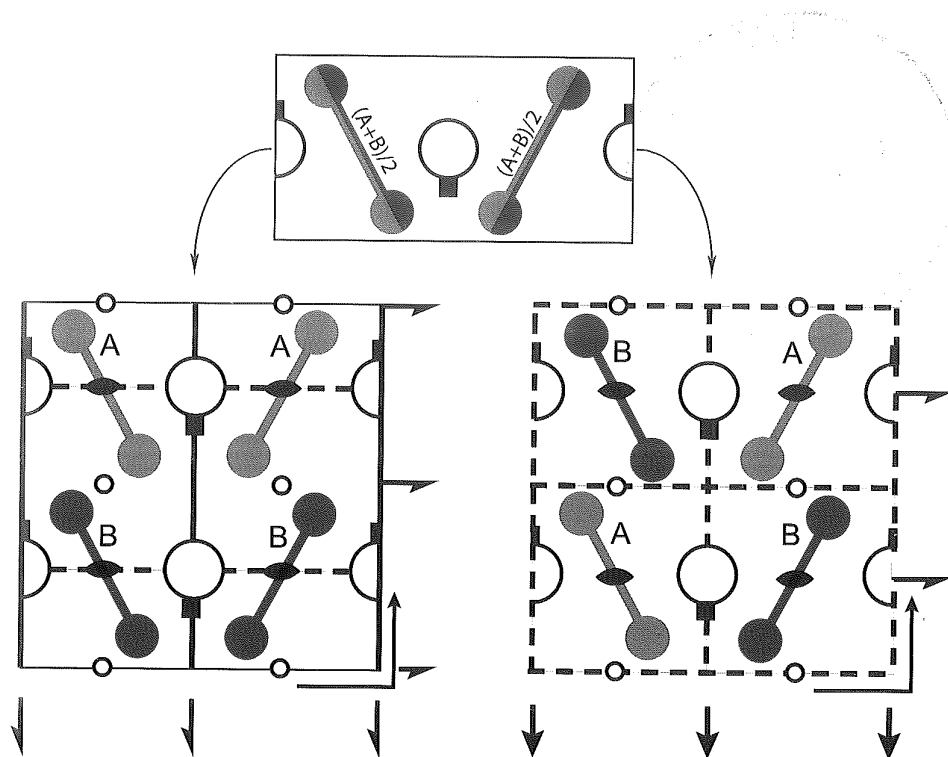
Diffuse Scattering

Edited by T. R. Welberry

Letter
T. L. Kuhl *et al.*: Grazing incidence diffraction at the solid-liquid interface

Oldenbourg